Experimental and numerical performance evaluation of building integrated photovoltaic with thermoelectric generator and phase change material

Yong-Kwon Kang [a], *Beom-Jun* Kim [a], *Soo-Jin* Lee [a], *Minseong* Kim [a], *Jae-Won* Joung [a], *Jae-Weon* Jeong [a].

[a] Department of Architectural Engineering, Hanyang University, Republic of Korea, kyk908525@hanyang.ac.kr

[a] Department of Architectural Engineering, Hanyang University, Republic of Korea, bumji21@hanyang.ac.kr

[a] Department of Architectural Engineering, Hanyang University, Republic of Korea, zkdie97@gmail.com

[a] Department of Architectural Engineering, Hanyang University, Republic of Korea, minseongk91@hanyang.ac.kr

[a] Department of Architectural Engineering, Hanyang University, Republic of Korea, jea4527@hanyang.ac.kr

[a] Department of Architectural Engineering, Hanyang University, Republic of Korea, jjwarc@hanyang.ac.kr

Abstract. Building-integrated photovoltaics (BIPVs) are the most promising systems for achieving zero-energy building in cities. However, BIPV has some shortcomings, such as a lack of solar tracking and a rapid increase in the PV surface temperature. Therefore, resolving these shortcomings requires system solutions to eliminate heat from panels or utilize heat sources to improve system efficiency. Heat dissipation methods using phase change materials (PCMs), heat fins, thermoelectric generators, air cooling, and water cooling have been proposed and studied. Among them, the passive technology PCM and thermoelectric generator are attracting attention. Using PCM can reduce the panel temperature without additional energy consumption. In addition, some studies have been conducted on BIPVs with a thermoelectric generator (TEG) or using a working fluid such as water or air to increase the system efficiency. Methods of heat recovery using fluids for conventional PV panels, owing to the characteristics of BIPVs installed on the exterior of building walls, have also been proposed. Some studies have also explored designs that combine TEGs, generating electric power depending on the temperature difference without additional equipment. However, TEGs also have the disadvantage of an extremely low power generation efficiency if they do not achieve a sufficient temperature difference. In this study, to address the shortcomings of each application, a BIPV combined with a PCM and TEG (BIPV-TEG-PCM) is proposed. Herein, the appropriate phase change temperature of the PCM and heat sink design in the PCM container were analyzed through computational fluid dynamics-based simulations and experiments.

Keywords. BIPV, Thermoelectric generator, PCM, Building-integrated photovoltaics, Phase-change material
DOI: https://doi.org/10.34641/clima.2022.216

1. Introduction

The increasing number of people living in cities [1] has led to the enormous energy consumption of buildings. The global Green New Deal requires high energy efficiency equipment and renewable energy. Nevertheless, the reality is that it is challenging to supply a large amount of renewable energy owing to the limited space in cities. Therefore, many studies have been conducted on building-integrated photovoltaics (BIPVs), solar panels integrated with building facades. However, BIPVs are fixed on the exterior building walls, unlike conventional PVs. Therefore, they have a limited time and angle for receiving sunlight. This disadvantage causing reduce the generation efficiency of PV panels. Various solutions have been proposed to improve the efficiency of the BIPVs (Fig 1) [2].

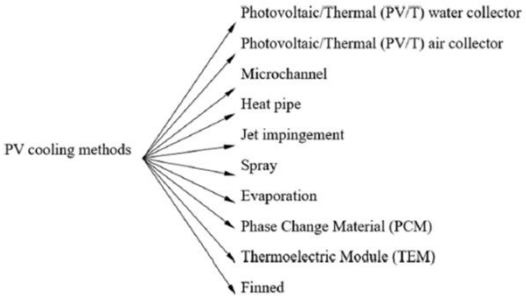

Fig. 1 - Cooling methods of PV panels.

Among the results of previous studies, the convection method had the best heat dissipation efficiency. Koyunbaba et al. (2013) proposed an air-cool-based BIPV thermal (BIPVT) system with a Trombe wall system [3]. An analysis based on the experiments and computational fluid dynamics (CFD) calculations showed that the average electrical and thermal efficiencies of this system could reach 4.52% and 27.2%, respectively. Kaiser et al. (2014) studied a BIPV module system under forced convection conditions [4]. Another study experimentally analyzed the influence of the air gap size and forced convection ventilation system. Under a duct velocity of 6 m/s, the power generation increased by 19% relative to the natural ventilation case. In addition, some studies have focused on water-cooling BIPVT systems. Kim et al. (2014) experimentally analyzed the energy performance of a water-cooled BIPVT integrated on a roof [5]. According to the experimental results, the average thermal and electrical efficiencies of the BIPVT were increased by 30% and 17%, respectively.

However, the fluid convection method is challenging to maintain and requires additional equipment and energy consumption to move the fluids. Therefore, research has been conducted on the BIPV system using a phase change material (PCM) and thermoelectric generator (TEG) to increase the efficiency passively. According to previous studies, the individual energy efficiency of the PV increased by 5.9% relative to that of an existing panel combined with PCMs [6]. Using a TEG, further development of approximately 5% was possible [7]. However, the PCM and TEG have low thermal conductivity and low generation efficiency. In addition, most preceding studies were insufficient considering the substantive problems of building-integrated PVs applied to buildings. Therefore, this study proposes a BIPV-TEG-PCM design considering practical installation, which combines the PV, PCM, and TEG. Furthermore, this study numerically and experimentally analyzed the optimal phase change temperature of the PCM, heat fin spacing, and TEG spacing for BIPV-TEG-PCM.

2. System and simulation overview

2.1 building integrated photovoltaic with thermoelectric generator and phase change material

Applying to the exterior surface of a building wall, BIPV-TEG-PCM is attached directly to the building wall. The integration with the wall using PCMs makes heat rejection possible without an additional power source or fluid for heat dissipation in the PV panel. Moreover, the BIPV-TEG-PCM does not cause infiltration or water-leakage problems from the exterior wall and prevents heat transfer to the interior side, reducing the heat load. The TEGs were located between the PV and PCM containers. The heat in the PV passes through the TEG during the day and is stored in the PCM container. Based on the Seeback effect, the TEG was generated electric power using the temperature difference generated at this time. The electricity generated from the PV and TEG is supplied to the necessary equipment through a battery or external circuit. In addition, the BIPV-TEG-PCM proposed in this study can generate energy at night. In the case of a PCM used to heat a PV during the day, recharging is required. Convection and longwave radiation from the PV surface decreased the surface temperature of the PV panel. The PCM was regenerated based on cooled PV. In this case, the reverse temperature difference between the PV and PCM containers allows the TEG to develop again. The temperature distributions in these processes are illustrated in Figures 1 and 2.

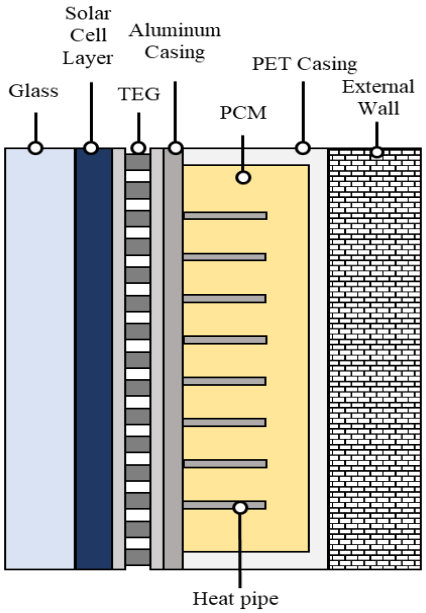

Fig. 2 - BIPV-TEG-PCM design.

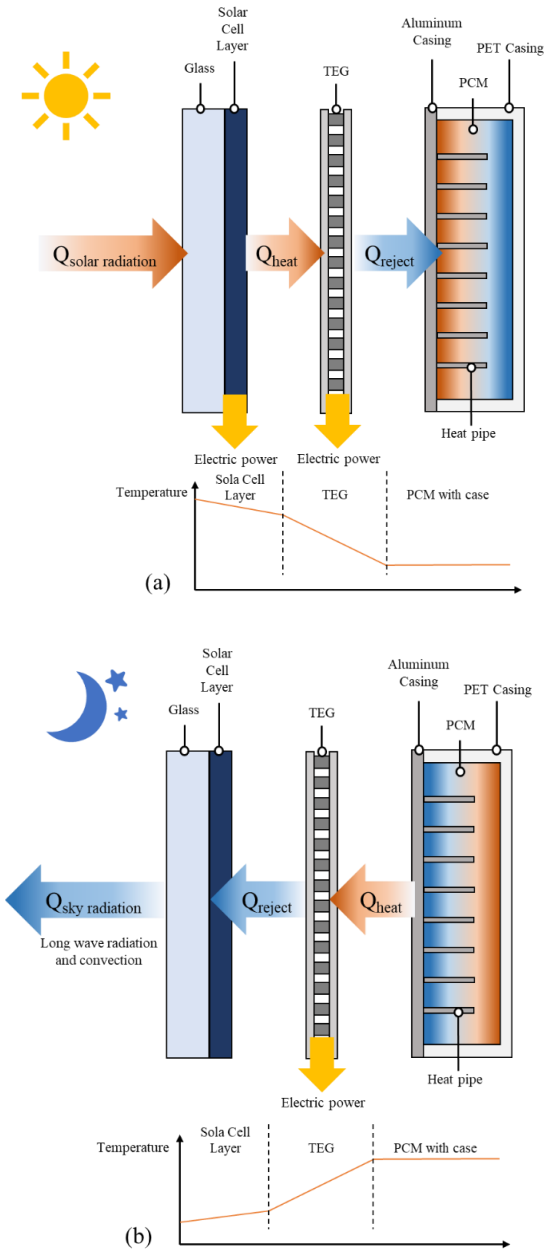

Fig. 3 - (a) BIPV-TEG-PCM operation during the daytime and (b) BIPV-TEG-PCM operation during the night.

2.2 Micro-encapsulated phase change material(mPCM)

In this study, the microencapsulated phase change material (mPCM) applied to easily manufacture and passively reject the heat from the PV panel. Moreover, a BIPV was installed on the outer skin of the building. Therefore, the use of the mPCM can prevent PCM leakage from the PCM container. Typical PCMs require precise containers because the particles are microscopic and easily leak from containers. In the case of mPCM, the particles are larger than the liquid-type PCM. The physical properties of the mPCM used in this simulation are listed in Table 1. Based on the results of the experiments in a preceding study [8], the selected ratio of PCM to tetrabutyl titanate (TBT) for the mPCM was as 6:4. Owing to the characteristics of the PCM, the material values vary slightly depending on the phase-change temperature. In addition, the material properties of the mPCM applied were fixed, and only the phase-change temperature was varied in the simulations.

Tab. 1 - Properties of n-eicosane micro-encapsulated PCM.

Property	Value
Density [kg/m3]	946.4
Specific heat [J/kgK]	1973.1
Latent heat [J/kg]	192660
Thermal conductivity [W/mK]	0.749
Melting point [℃]	25, 35 45
Particle size [μm]	10

3. Experimentation and simulation overview

3.1 Experiment overview

This experimentation conducted on the roof of a building located in Seoul in summer. In this experiment, the surface temperature of the PV panel was compared which the PCM was integrated and the panel without PCM. To monitor the temperature variation of each layer, T-type thermocouples were attached at the PV panel surface, TEG cold side and interior of PCM.

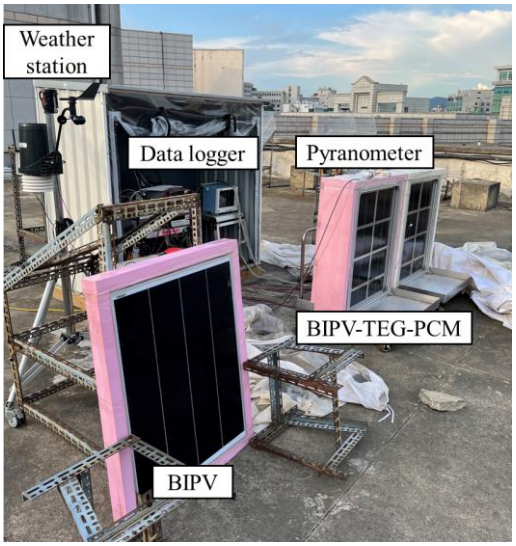

Fig. 4 - Figure caption.

3.2 CFD simulation overview

Transient simulations were conducted using ANSYS FLUENT, a commercially available software package. The purpose of this simulation was to identify the PCM at an appropriate phase-change temperature.

In addition, the PCM used in this study was mPCM in powder form; therefore, the calculation was conducted by assuming a laminar flow because there was no fluid. In addition, most of the heat is transferred within the BIPV-TEG-PCM through conduction. A CFD mesh was constructed using a two-dimensional model. The physical properties of the PCMs used in the CFD settings are listed in Table 1, and other material physical properties are described in previous studies [9–11]. In this simulation, several assumptions were made to reduce the computational time and compare the results in the same environment, and the properties of all objects are unaffected by time and temperature changes. The effects of natural convection were ignored in the PV panel surface. The project was simulated with a size smaller than the actual size.

The total number of nodes was 14,864 (Fig. 5). Based on the PV standard test (STC) conditions of 25 °C and 1000 W/m^2, the heat flux to the PV panel surface was fixed at 1000 W/m^2, and the other surfaces were set under insulation conditions. The total simulation time was four h (i.e., 14400 s), and the results were plotted every second. The properties of the other materials are listed in Table 2.

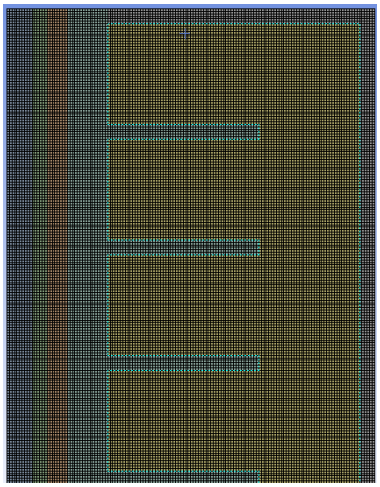

Fig. 5 - Figure caption.

Tab. 2- Properties of BIPV-TEG-PCM.

Material	Density [kg/m3]	Specific heat [J/kgK]	Thermal conductivity [W/mK]
PV	2230	700	148
Aluminium	2719	871	202.4
PET	1500	1200	0.2
TEG	7670	198	1.61

4. Results

4.1 Simulation results

In this study, simulation analysis was performed on heat fin spacing for PCM container, melting temperature of PCM, and TEG spacing to derive an appropriate BIPV-TEG-PCM design. In addition, an outdoor experiment was conducted using a prototype.

The result of optimal heat fin spacing is shown in figure 6 below. In this study, a total of 5 spacings of no fin, 5, 10, 20, and 30 mm were analyzed, and the surface temperature of the PV panel with 5 mm heat fin spacing cases were compared in each PCM melting temperature (i.e., 25, 35 and 45°C). As a result of the simulation, it was found that the 20 mm heat fin spacing could maintain the lowest panel surface temperature regardless of the PCM melting temperature. If the fin spacing is tight, heat transfer is improved, and rapid heat transfer to the PCM is possible. However, due to the decreased amount of the PCM, the melting area of PCM was crated faster than wide fin spacing. Therefore, results showed a faster temperature rise compared to the other fin interval. This phenomenon appeared more clearly as the melting temperature of the PCM was lower, and when the melting temperature of the PCM was increased, a better effect was shown based on rapid heat transfer.

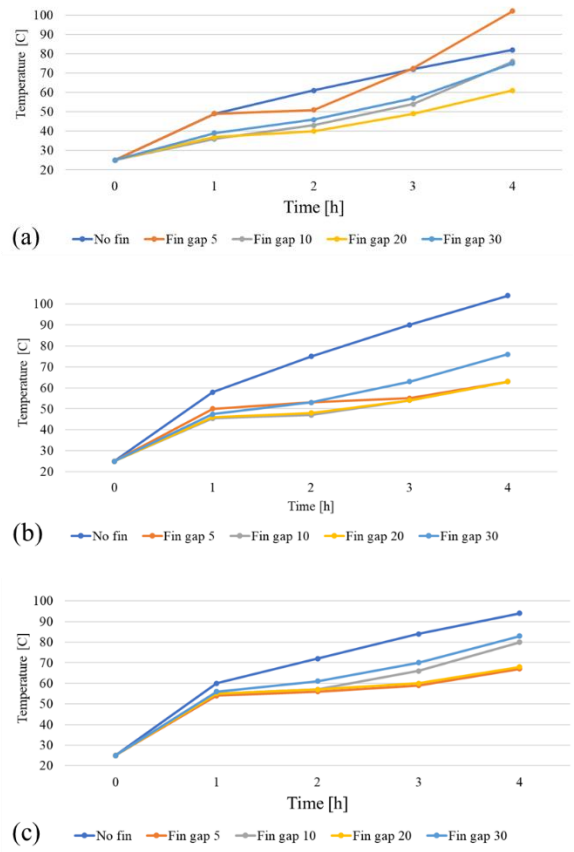

Fig. 6 – PV surface temperature comparison: (a) heat fin spacing with PCM 25 (b) heat fin spacing with PCM 35 and (c) heat fin spacing with PCM 45.

The appropriate PCM melting temperature was compared in each heat fin interval (Fig. 7). As a result of the simulation, the PCM melting

temperature of 25°C shows the best performance for the low PV surface temperature in each case. However, in the case of the close interval heat fin spacing of 5 and 10 mm with PCM 25°C, it was kept low for the first two hours, after two hours showed a steeper temperature rise as the phase change progressed. On the other hand, the high melting temperature PCM with a high temperature showed a similar pattern of increasing gradually at both 35 and 45°C. When the heat fin spacing was narrow, the PCM 35°C showed better performance than PCM 25°C.

Therefore, there may be different combinations depending on the conditions of use. However, using a PCM melting temperature 25°C can maintain the lowest panel surface temperature in STC conditions.

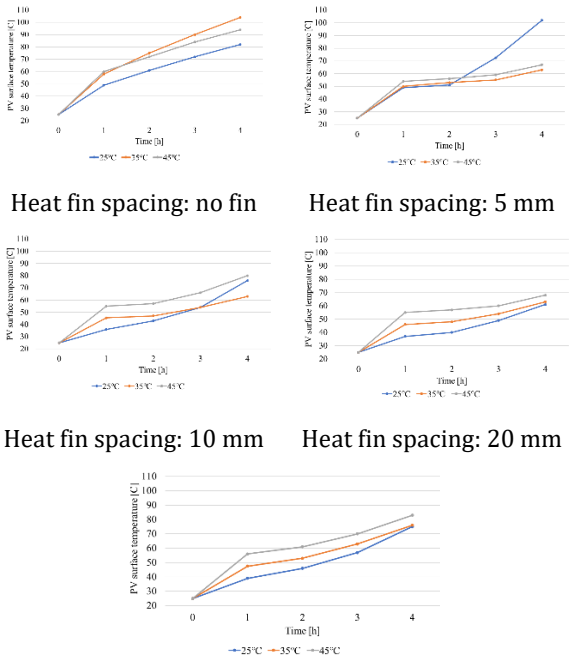

Fig. 7 - PV surface temperature distribution with different melting temperature of PCM.

As shown in figure 8, four TEG intervals were selected for simulation (i.e., 70, 93, 140, and 280 mm). As a result of the TEG spacing simulation, it was found that the temperature difference between the cold and hot sides of the TEG increased as the TEG interval widened. In addition, the panel surface temperature distribution of the remaining cases except for 280 mm was a similar pattern, and it was found that the largest temperature difference occurred when the thermoelectric element was spaced at 140 mm. Therefore, the most appropriate TEG spacing is determined to be 140 mm. The heat transfer rate of the TEG is larger than PCM. Therefore, the closer the distance of the TEG cause, the more heat transfer to the PCM and heat fin. Therefore, it causes the unbalance heat transfer rate between PV to TEG and TEG to PCM. Therefore, the temperature of the cold side and hot side of TEG show similar temperatures.

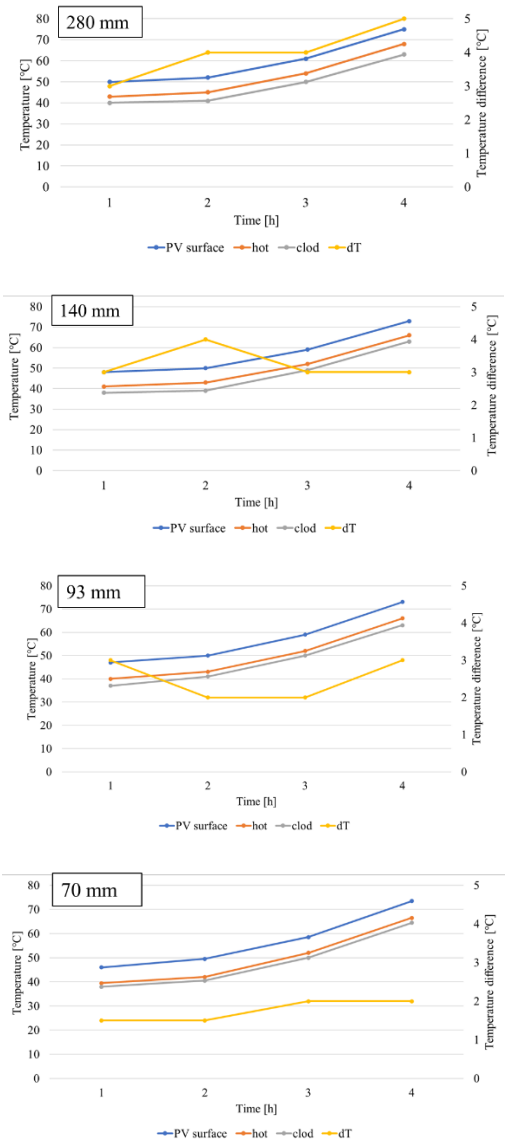

Fig. 8 - PV surface temperature distribution with different TEG interval.

4.2 Experimentation results

As a result of the experiment (Fig. 9), PV surface temperature at the peak was about 20°C lower with the PCM than the panel without the PCM. However, there was no significant difference in surface temperature of the PV panels between the PCM melting temperature at 35°C and 45°C. Therefore, using the PCM and TEG with the PV panel can improve the 13% of PV panel efficiency. As a result of the measurement, it was confirmed that eight TEGs could produce a total of 0.04 Wh of electricity per day. In addition, the amount of power generation changes according to the insolation was confirmed following the characteristic of TEG (Fig. 10).

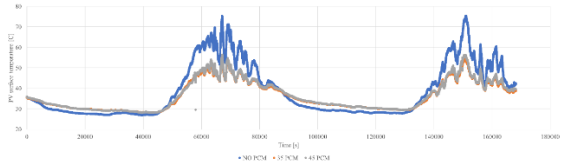

Fig. 9 - PV surface temperature measurement by prototype experiment.

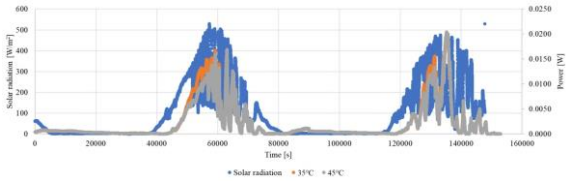

Fig. 10 - TEG power generation during the summer.

5. Conclusion

This study analyzed the impact of the phase change temperature, the heat fin, and TEG arrangement on thermal behavior through CFD transient simulations. In addition, prototype experimentation of the BIPV-TEG-PCM system was conducted to confirm the effect of reducing PV surface temperature by the PCM. As a result of simulation, low phase change temperature helps inhibit an early temperature rise. However, it has been shown that high melting temperature PCM maintain similar or low temperatures for a more extended period if there is a proper design heat fin spacing. Therefore, using a suitable melting temperature PCM with the proper heat fin spacing can increase the efficiency of the panel, which can further contribute to a zero-energy building. In addition, as shown in the experiment results, the PCM can reduce the PV surface temperature by about 20°C lower than the PV panel without the PCM.

Thus, the further study intents to manufacture the second experimental unit of BIPV-TEG-PCM and verify the simulation results through outdoor experiments.

Acknowledgement

This work was supported by Korea Institute of Energy Technology Evaluation and Planning (KETEP) grant funded by the Korea government (MOTIE) (No. 20202020800360), and this work was supported by the Korean Agency for Infrastructure Technology Advancement (KAIA) grants (21CTAP-C163749-01).

6. References

[1] Programme UNE, Construction GA for B and. 2020 Global Status Report 2020.

[2] Bayrak F., Oztop HF., Selimefendigil F. Experimental study for the application of different cooling techniques in photovoltaic (PV) panels. Energy Convers Manag 2020;212:112789.

[3] Koyunbaba BK., Yilmaz Z., Ulgen K. An approach for energy modeling of a building integrated photovoltaic (BIPV) Trombe wall system. Energy Build 2013;67:680–8.

[4] Kaiser AS., Zamora B., Mazón R., García JR., Vera F. Experimental study of cooling BIPV modules by forced convection in the air channel. Appl Energy 2014;135:88–97.

[5] Kim JH., Park SH., Kang JG., Kim JT. Experimental performance of heating system with buildingintegrated PVT (BIPVT) collector. Energy Procedia 2014;48:1374–84.

[6] Hasan A., Sarwar J, Alnoman H, Abdelbaqi S. Yearly energy performance of a photovoltaic-phase change material (PV-PCM) system in hot climate. Sol Energy 2017;146:417–29.

[7] Makki A. Innovative heat pipe-based photovoltaic/thermoelectric (PV/TEG) generation system. PhD Thesis Univ Nottingham 2017:329.

[8] Chai L., Wang X., Wu D. Development of bifunctional microencapsulated phase change materials with crystalline titanium dioxide shell for latent-heat storage and photocatalytic effectiveness. Appl Energy 2015;138:661–74.

[9] Liu XD., Park YH. Structure and transport properties of (Bi1-xSbx)2Te3 thermoelectric materials prepared by mechanical alloying and pulse discharge sintering. Mater Trans 2002;43:681–7.

[10] Niu X., Yu J., Wang S. Experimental study on low-temperature waste heat thermoelectric generator. J Power Sources 2009;188:621–6.

[11] Kazemian A., Salari A., Ma T. A year-round study of a photovoltaic thermal system integrated with phase change material in Shanghai using transient model. Energy Convers Manag 2020;210:112657.